A Dual-Emission Förster Resonance Energy Transfer Nanoprobe for Sensing/Imaging pH Changes in the Biological Environment

Ya-Ling Chiu,[†] Show-An Chen,[†] Jean-Hong Chen,[‡] Ko-Jie Chen,[†] Hsin-Lung Chen,[†,*] and Hsing-Wen Sung[†,*]

[†]Department of Chemical Engineering, National Tsing Hua University, Hsinchu 30013, Taiwan, and [‡]Department of Polymer Materials, Kun Shan University, Tainan 71003, Taiwan

ABSTRACT A dual-emission nanoprobe that can sense changes in the environmental pH is designed based on the concept of pH-responsive Förster resonance energy transfer induced by the conformational transition of an associating polyelectrolyte, *N*-palmitoyl chitosan, bearing a donor (Cy3) or an acceptor (Cy5) moiety. We demonstrate that the developed pH-responsive nanoprobe can be used to ratiometrically image and thus discriminate the pH changes in the biological environment at different length scales.

KEYWORDS: pH-responsive nanoprobe · Förster resonance energy transfer · ratiometric imaging · dual emission · associating polyelectrolyte · nanostructure transformation

Stimuli-responsive materials have been receiving much attention due to their potential applications in biomedicine; in particular, those capable of probing environmental changes, such as pH and temperature, have been extensively sought for detecting biological phenomena intracellularly or extracellularly. Intracellular pH is generally between 6.8 and 7.4 in the cytosol and between 4.5 and 6.0 in the cell's acidic organelles.[1] When compared with conventional microelectrode techniques, fluorescent dyes provide an enhanced sensitivity required for optical pH measurements inside living cells and offer a greater spatial sampling capability. However, the optical change of fluorescent dyes is often relatively small and monotonous (in single-emission pattern), thus limiting their roles in probing intracellular pH changes.[2,3] This highlights the need to develop improved fluorescent probes that can sense pH changes intracellularly. On the other hand, many pathological conditions, such as cancers, are associated with increased metabolic activity and hypoxia, resulting in an elevated extracellular acidity.[4,5] Imaging acidic regions could provide valuable information about disease localization and progression and might enhance diagnosis and therapy. Therefore, developing a pH-responsive fluorescence probe that can be used for detecting variations in the environmental acidity is of significant interest.

In this study, a dual-emission nanoprobe that can sense changes of the environmental pH is developed based on the concept of pH-responsive Förster resonance energy transfer (FRET) of a biocompatible polyelectrolyte, *N*-palmitoyl chitosan (NPCS), conjugated with a donor (Cy3) or an acceptor (Cy5) moiety (Figure 1). FRET involves the nonradiative transfer of energy from an excited-state fluorophore (donor) to a second chromophore (acceptor) in a close proximity (less than 10 nm).[6−8] FRET measurements offer a highly effective means of probing either molecular interactions or a single molecular event, such as molecular cleavage and conformational transition of a protein, thus providing a platform to design a sensor molecule for detecting the variation in molecular environments.[9−14] FRET imaging that allows the simultaneous recording of two emission intensities at different wavelengths in the presence or absence of analytes has provided a feasible approach for visualizing a complex biological process at the molecular levels.[15] Therefore, developing dual-emission fluorescent probes provides ratiometric measurements of the emission intensities by modulating a FRET process.

RESULTS

Our central idea is schematically illustrated in Figure 1. NPCS is an associating polyelectrolyte characterized by the presence of alternating charges (protonated

*Address correspondence to hwsung@che.nthu.edu.tw, hlchen@che.nthu.edu.tw.

Received for review October 5, 2010 and accepted November 12, 2010.

Published online November 17, 2010. 10.1021/nn102644u

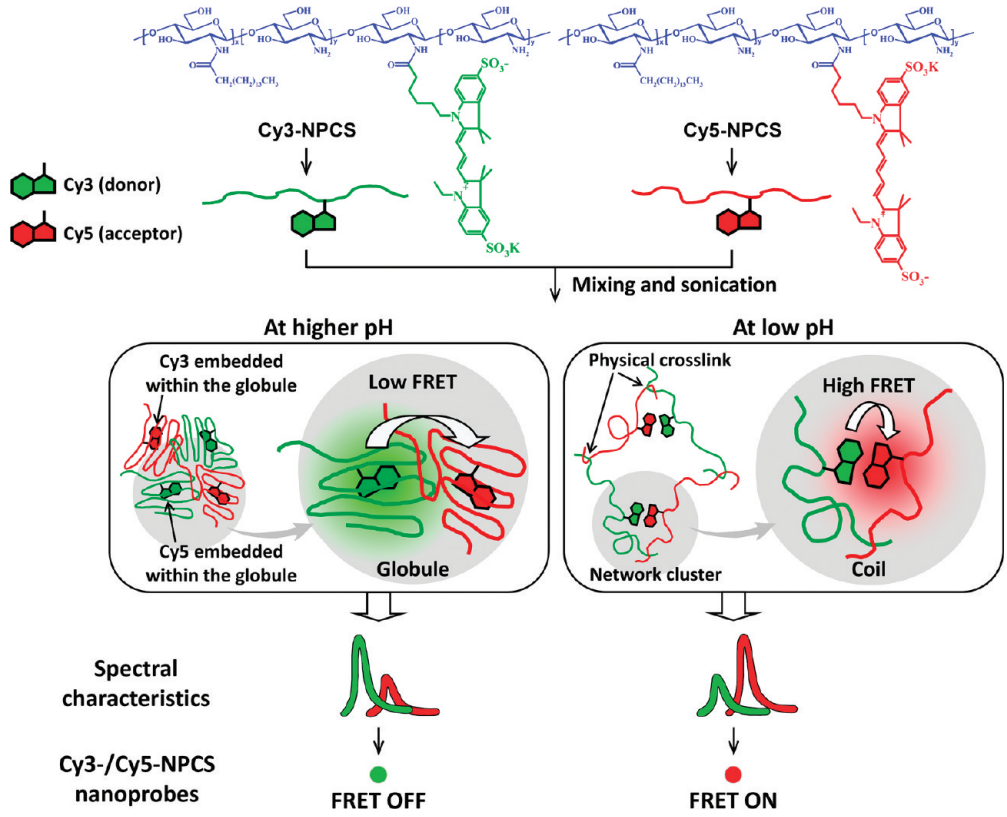

Figure 1. Design and working principle of the pH-responsive FRET nanoprobes. Schematic illustrations showing a dual-emission nanoprobe that can sense changes of the environmental pH, based on the concept of pH-responsive FRET of a biocompatible polyelectrolyte, NPCS, conjugated with a donor (Cy3) or an acceptor (Cy5) moiety.

amine groups) and hydrophobic side chains (palmitoyl groups). We have shown previously that NPCS in an aqueous environment exhibits a rapid nanostructure transformation within a narrow pH range through a proper balance between charge repulsion and hydrophobic interaction.[16] Here we further attach a tiny amount of Cy3 or Cy5 moiety to the backbone of NPCS to yield Cy3−NPCS and Cy5−NPCS, respectively. The molar ratio of Cy3 or Cy5 to NPCS monomers was *ca.* 0.4%; therefore, a NPCS chain contained about one Cy3 or Cy5 group as estimated from the polymer molecular weight. Cy3−NPCS and Cy5−NPCS in equal amounts were added into the aqueous solution with a prescribed pH to yield the solutions containing the mixture of these two species. It has been shown that the NPCS with a sufficiently high degree of substitution (DS, *e.g.* 15%) of palmitoyl group would form nanoscale network clusters [which will be called "nanoparticles (NPs)" hereafter] at low pH, where a fraction of the hydrophobic side chains associated to form micellar aggregates that acted as the physical cross-links tying NPCS chains to generate the network.[16] The NPCS chains between the physical cross-links were highly expanded due to charge repulsion between the protonated amine groups on the backbone. Our quantitative analysis of the small-angle X-ray scattering profile associated with these network clusters revealed that the characteristic mesh size of the network was in the order of 2 nm.[16] As a result, in the network clusters containing both Cy3−NPCS and Cy5−NPCS chains, Cy3 and Cy5 moieties are well exposed to each other, and their separation distance should lie within the critical distance (~10 nm) required for FRET. An energy transfer from Cy3 to Cy5 is hence expected to take place at low pH. When pH is raised, the increase in hydrophobicity of NPCS arising from deprotonation of the amine groups induces the collapse of polymer chains into globules. Once the intrachain collapse dominates, Cy3 and Cy5 moieties will be embedded within the individual globules and hence will become inaccessible to their counterpart for energy transfer. Consequently, the ability of NPCS to self-associate to form expanded network clusters offers the close proximity between the donor and the acceptor moieties required for FRET, while the pH-driven conformational transition prescribes the on-to-off switch of the energy transfer.

NPCS was prepared by conjugating a hydrophobic palmitoyl group onto the free amine groups of chitosan (CS). CS, a natural-origin polysaccharide, is biodegradable, nontoxic, and soft-tissue compatible and thus has been used extensively in biomedical applications.[17] It is known that the pK_a of CS is approximately 6.5.[17,18] The pH-triggered conformational transition was demonstrated by comparing the hydrodynamic radii (R_h) of NPCS with a DS of 15% (denoted as NPCS-15%) at pH 4.5 and 7.4, measured by dynamic light scattering at

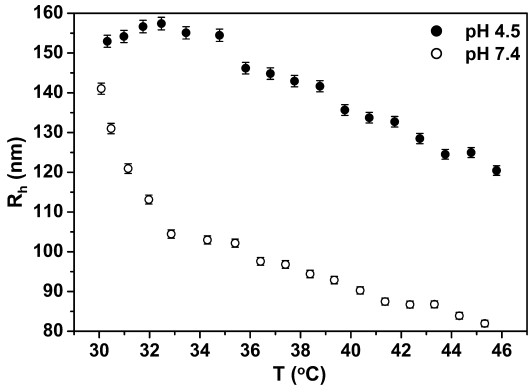

Figure 2. Hydrodynamic radii (R_h) of test nanoparticles prepared by NPCS with a degree of substitution of 15% at pH 4.5 and 7.4, measured by dynamic light scattering at varying temperatures.

varying temperatures (Figure 2). It can be seen that R_h at pH 4.5 was always greater than that at pH 7.4 under a given temperature. At the physiological temperature (*ca.* 37 °C), for instance, R_h at pH 4.5 was 145 nm as compared to 97 nm at pH 7.4. It is noted that the size of NPs measured was significantly larger than that expected for single polymer chains (at the order of several nm), thereby confirming that aggregates or clusters of NPCS were formed in aqueous media.

Figure 3a shows the FRET spectra of Cy3−/Cy5−NPCS-15% NP solutions, which were normalized to the maximum Cy3 donor peak around 570 nm, as a function of the environmental pH; their corresponding emission ratio of Cy5/Cy3 is shown in Figure S1 of the Supporting Information. All spectra were obtained by irradiating solutions at 520 nm, corresponding to the excitation wavelength of the FRET donor, Cy3. As the environmental pH was changed, spectral changes were observed; sequential increases in the fluorescence emission ratio of Cy5/Cy3 were observed with decreasing the pH. The increase in the emission ratio of Cy5/Cy3 was due to a higher FRET efficiency; that is, more energy transferred from Cy3 to Cy5 at lower pH. The variation in the FRET efficiency with pH values was consistent with our postulated mechanism of the pH-triggered NPCS conformational change. This accordance implies that intrachain collapse of NPCS in the network clusters at higher pH should take place predominantly; in this case, Cy3 and Cy5 moieties were located at different globules such that their mutual interactions required for energy transfer were effectively shielded. If interchain collapse was the dominated mode, then a single globule would have contained both Cy3 and Cy5 moieties, and hence energy transfer was still accessible. It is interesting to note that some Cy5 emission still existed at pH 8.0 (Figure 3a). This may be due to the presence of some Cy3 and Cy5 groups at the surface of the collapsed aggregates, such that a small fraction of Cy3 moiety was still able to interact with Cy5 to induce the energy transfer.

It is noted that Cy3−/Cy5−NPCS with a DS of 15% represented the optimum prescription for attaining high FRET efficiency. NPCS with a lower DS was found to display lower FRET efficiency (see Supporting Information, Figure S2), given that the polymer chains could not form clusters effectively in aqueous media at lower pH due to a weaker hydrophobic interaction. In this case, a significant fraction of chains remained well dispersed, and their large separation distance at low polymer concentration (100 μg/mL) frustrated the energy transfer from the Cy3 groups in a given chain to the Cy5 groups in others. On the other hand, the variation in size for the NPs prepared from NPCS with a DS larger

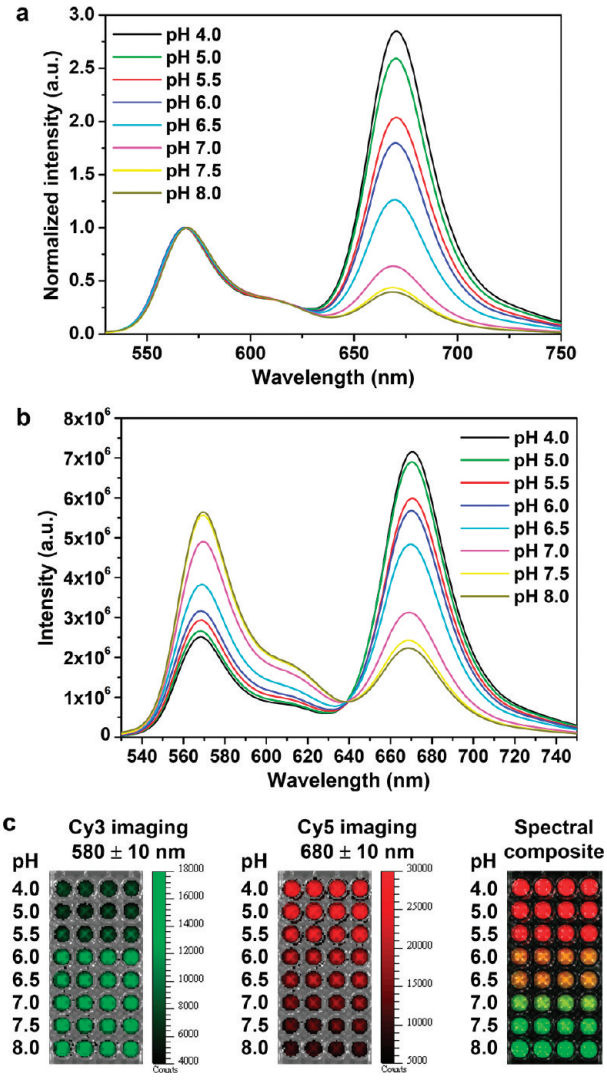

Figure 3. FRET measurements. (a) FRET spectra of Cy3−/Cy5−NPCS-15% nanoparticle suspensions, which were normalized to the maximum Cy3 donor peak around 570 nm, as a function of environmental pH and (b) the corresponding non-normalized FRET spectra; (c) dual-emission pH images of Cy3−/Cy5−NPCS-15% nanoparticle suspensions obtained by an *in vivo* imaging system. All of FRET spectra and dual-emission pH images were obtained by irradiating nanoparticle suspensions at 520 and 535 ± 15 nm, respectively, corresponding to the excitation wavelength of the FRET donor, Cy3. NPCS-15%: NPCS with a degree of substitution of 15%.

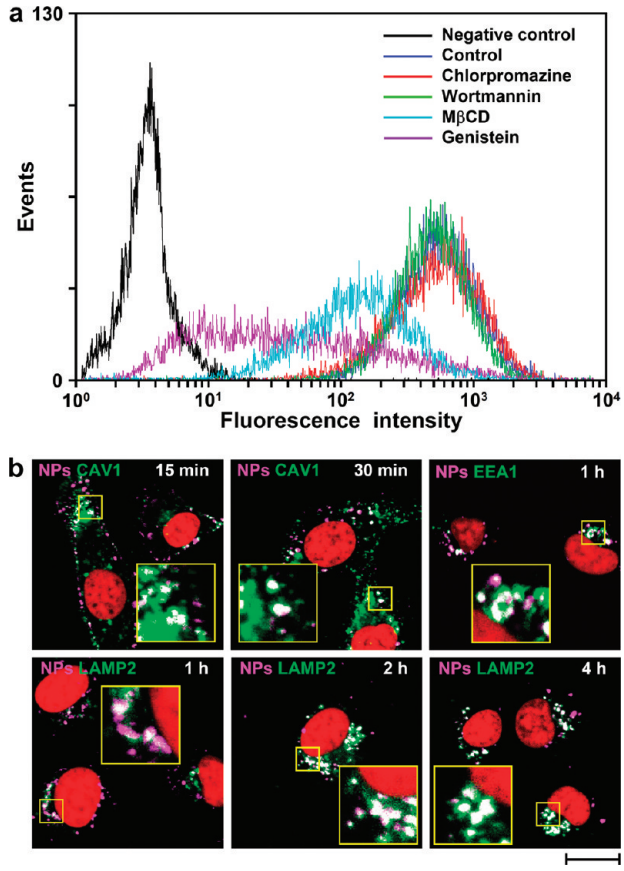

Figure 4. Endocytosis pathway and intracellular trafficking. (a) Effects of inhibitors on the internalization of NPCS NPs in the presence of chlorpromazine (7 μg/mL), wortmannin (500 nM), MβCD (3 mM), or genistein (200 μM). Negative control: the group without any treatment; control: the counterpart in the absence of inhibitors; and NPCS NPs: nanoparticles of NPCS with a degree of substitution of 15%. (b) Confocal images (scale bar, 20 μm) of the intracellular trafficking of NPCS NPs taken at the indicated time points using the immunohistochemical stains to identify caveolae/caveosomes (CAV1), early endosomes (EEA1), and late endosomes/lysosomes (LAMP2). Area defined by a square is shown at a higher magnification in the inset.

than 15% became significant; therefore, they were not used in the study.

Figure 3b shows the non-normalized FRET spectra of Cy3−/Cy5−NPCS-15% NP suspensions. With decreasing the pH, concomitant systematic increases in Cy5 emission and decreases in Cy3 emission, due to an increase in Cy3 to Cy5 FRET, were observed. This pH-dependence phenomenon allows the ratio of fluorescence intensities emitted from the donor and acceptor dyes at two emission wavelengths (570 and 670 nm) to be used for quantitative determinations of pH. Figure 3c shows the dual-emission pH images obtained by an *in vivo* imaging system (IVIS). Cy3 and Cy5 images were acquired through 580 ± 10 and 680 ± 10 nm band-pass emission filters, respectively. When Cy3−/Cy5−NPCS-15% NP suspensions were excited at 535 ± 15 nm, the fluorescent intensity of the Cy3 band decreased gradually, and the Cy5 band increased with decreasing pH. As a result, an obvious change in fluorescent ratio color imaging (spectral composite) from green (pH 7.5) to orange (pH 6.0) and then red (pH 5.0) was observed. These ratiometric images may be used to discriminate the environmental pH changes at a length scale related to the pathological acidic regions in tissues, thus providing valuable information about the disease localization and progression.

The aforementioned results suggest that the developed Cy3-/Cy5-labeled NPCS NPs can be used as a dual-emission nanoprobe for detecting variations in the environmental acidity, especially in the pH ranges of 7.5−4.0. Moreover, the environmental pH can be imaged from the ratio of signal intensity of Cy3 (FRET donor) and Cy5 (FRET acceptor) on NPCS *via* modulating a pH-responsive FRET process. Further, this technique was demonstrated in a cell model to access the possibility of using the developed Cy3-/Cy5-labeled NPCS NPs to probe, image, or discriminate varied acidity of cellular organelles.

To elucidate their potential cellular uptake pathway, the interaction between NPCS-15% NPs (fluorescein-labeled) and cell membranes was investigated by treating cells (HT1080 human fibrosarcoma) with different chemical inhibitors and then analyzed by flow cytometry; the counterparts in the absence of inhibitors were used as controls. Chlorpromazine and wortmannin have been used as inhibitors for clathrin-mediated uptake and macropinocytosis, respectively.[19−22] As shown in Figure 4a, treatment with chlorpromazine or wortmannin did not result in a significant inhibition of uptake of NPCS NPs, indicating that neither clathrin-mediated endocytosis nor macropinocytosis was involved in the endocytosis. Methyl-β-cyclodextrin (MβCD) and genistein are known to inhibit caveolae-mediated endocytosis, each acting by a different mechanism.[19−22] As compared to the control, cells treated with MβCD or genistein significantly diminished the fluorescence intensity, an indication of caveolae-mediated endocytosis. The aforementioned results suggest that the caveolae-mediated pathway played a significant role in the internalization of NPCS NPs.

Caveolae are characterized by the presence of a family of caveolin proteins including caveolin-1 (CAV1).[23,24] To further support the entry of NPCS NPs *via* the caveolae-mediated pathway, the potential colocalization of CAV1 and test NPs during and after entry into cells was investigated. As shown in Figures 4b and S3 (in the Supporting Information), NPCS NPs were initially observed in cell membranes and colocalized with CAV1 (caveolae marker, at 15 min after incubation). The internalized NPs were found associated with CAV1-positive structures (caveosomes, at 30 min after) near the cell periphery. Subsequently, significant levels of NPs were found colocalized with early endosomes (EEA1, at 1 h after); the early endosomes then matured into late endosomes and then to lysosomes at longer incubation time points (1 to 4 h, LAMP2). These data demonstrate

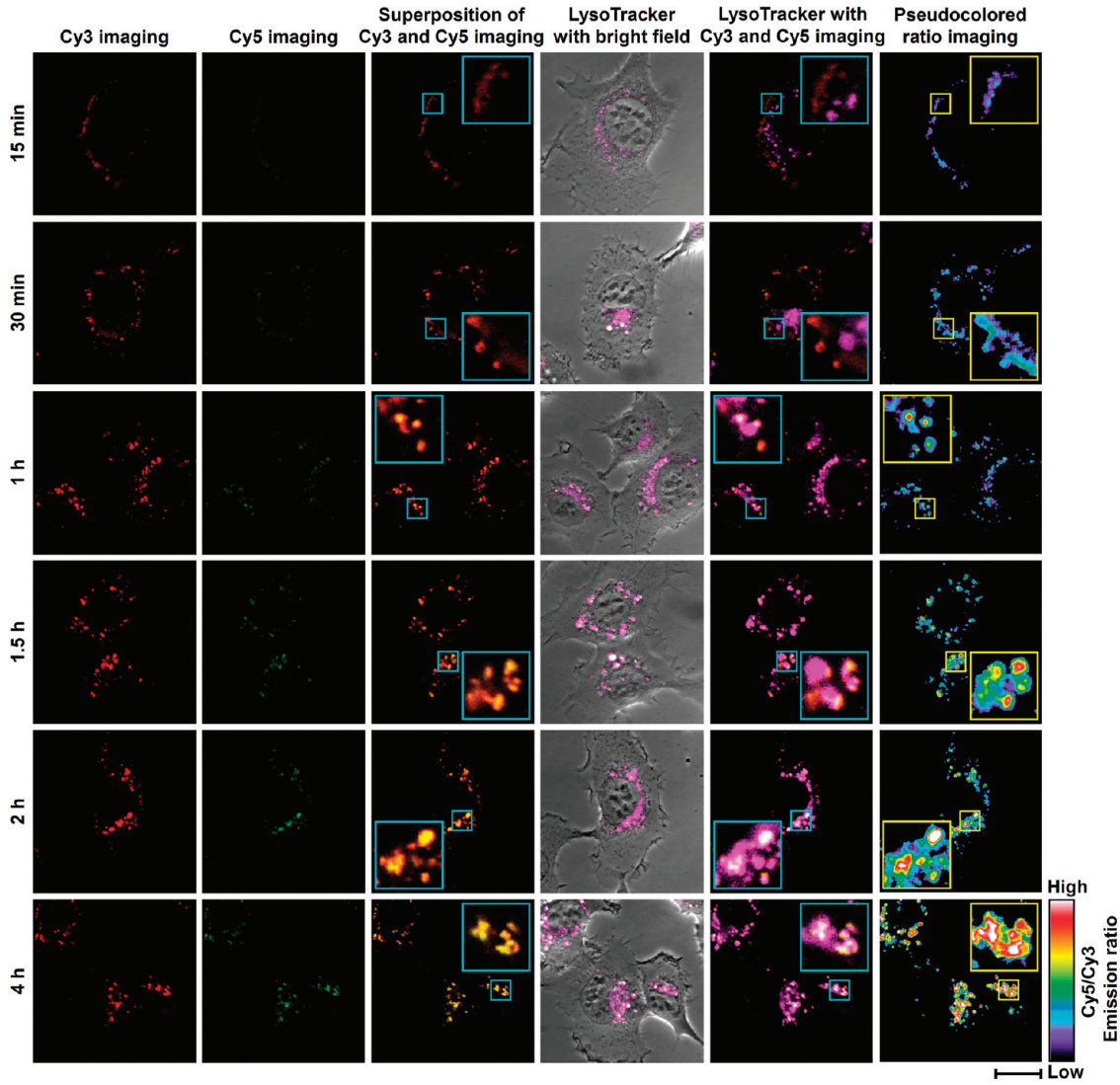

Figure 5. Mapping spatial pH changes in living cells. Dual-emission fluorescence images (scale bar, 20 μm) of cells treated with Cy3−/Cy5−NPCS NPs for distinct durations taken by a confocal laser scanning microscope by irradiating NP suspensions at 543 nm. The fluorescence images were acquired in optical windows between 560−600 nm (Cy3 imaging channel) and 660−700 nm (Cy5 imaging channel). The corresponding pseudocolored ratio images were obtained by analyzing the ratio of the signal intensities of Cy5 to Cy3 imaging channels. NPs: nanoparticles of NPCS with a degree of substitution of 15%.

that following the caveolar endocytosis, NPCS NPs traffic within early endosomes, which mature into acidic late endosomes and lysosomes.

The feasibility of using the prepared fluorescent (Cy3-/Cy5-labled) NPCS NPs to probe the intracellular acidic organelles (early endosomes, late endosomes and lysosomes) was evaluated. Cells were incubated with Cy3-/Cy5-labled NPCS NPs for distinct durations, and fluorescence images were then taken by a confocal laser scanning microscope (CLSM) (Figure 5) in optical windows between 560−600 nm (Cy3 imaging channel) and 660−700 nm (Cy5 imaging channel) when irradiating NP suspensions at 543 nm. By 15 min after treatment, fluorescence was already observed in the Cy3 imaging channel; in contrast, no fluorescence was observed in the Cy5 imaging channel until 1 h after incubation. With time progressing, the intensity of intracellular fluorescence seen in the Cy5 imaging channel became stronger. The superposition of Cy3 and Cy5 imaging (the third column in Figure 5) changed apparently from red (15 to 30 min, FREF off), to orange (1 to 1.5 h, FRET on) and then yellow (2 to 4 h) due to an increase in FRET from Cy3 to Cy5 over time. This indicates that after cellular internalization, test NPs may traffic intracellularly from neutral (caveosomes, 30 min) to acidic organelles [early endosomes (1 h) and late endosomes/lysosomes (2 to 4 h)], which is consistent with the results observed in Figure 4b.

A LysoTracker (Yellow-HCK-123) probe, a fluorescent acidotropic probe, was used as a control for labeling acidic organelles in cells (the fourth column in Figure 5), and their images were acquired in optical windows between 500−540 nm. As early as 15−30 min after incubation, intracellular acidic organelles were already stained by LysoTracker (indicated in purple); however, the color of LysoTracker was monotonous

throughout the entire course of the study (up to 4 h). In contrast, at 15−30 min after incubation, the internalized test NPs (stained in red, the fifth column in Figure 5) were still at cell membranes or near the cell periphery. At this time, no apparent colocalization of test NPs with LysoTracker was observed; therefore, the red color shown in Cy3/Cy5 images (the third column in Figure 5, FRET off) represents a neutral pH environment (caveosomes). After incubation for 1 h, test NPs were found in colocalization (in white) with the organelles stained by LysoTracker, and their color turned to orange (the third column in Figure 5, FRET on), indicating their trafficking into the weakly acidic early endosomes. At a later time point (1.5 h after), the color of test NPs (colocalized with LysoTracker) changed gradually again from orange to yellow, suggesting that NPs were conveyed from early endosomes to more acidic organelles (late endosomes or lysosomes). With time progressing (2 to 4 h), this phenomenon was more remarkable, an indication of the accumulation of test NPs in lysosomes.

Variations in the intracellular acidity can be further evaluated using the ratio of the signal intensities of Cy5 to Cy3 imaging channels analyzed by ZEN 2009 Light Edition Software; the obtained Cy5/Cy3 emission ratio is represented by a range of pseudocolors presented in the last column in Figure 5. As shown, the Cy5/Cy3 emission ratio in cells varied with time after the internalization of test NPs. With time increasing, stimulated by the decrease in intracellular pH, an increase in the Cy5/Cy3 emission ratio was observed, an indication of a higher FRET efficiency. The higher FRET efficiency seen in a lower pH environment was induced by the pH-triggered NPCS conformational change, as discussed above. The aforementioned results demonstrate that the developed Cy3-/Cy5-labeled NPCS NPs can be used effectively as a ratiometric fluorescent pH-sensor for probing the acidity of endocytic organelles in live cells. This feature is advantageous over the traditional fluorescent acidotropic probe (LysoTracker), which can only display a monotonous color and is therefore not able to distinguish the variation in environmental pH in intracellular organelles.

DISCUSSION

Development of a sensitive and practical means for the detection of environmental pH changes is essential in addressing the challenges in locating intracellular acidic organelles and acidified morbid tissues. FRET is a powerful technique in optical imaging; it substantially improves the performance of the conventional florescence-based probes, which displays merely single-emission patterns with a modest change in fluorescence intensity when responding to the environmental stimuli. A few FRET-based pH sensing methods, including conjugating/entrapping a pH-sensitive fluorescent dye on quantum dots or in nanogels, have been reported in the literature;[25−27] however, their pH sensitive capacity is limited to 6.0−8.0, thus restricting their biological applications below pH 6.0.

To address this concern, we develop a dual-emission FRET nanoprobe made of NPCS for sensing pH changes in the biological environment. With the modulation of their conformational transition in response to the environmental pH changes, the gradual alteration in accessibility of the donor (Cy3) to the acceptor (Cy5) on NPCS for energy transfer contributes to different FRET efficiencies. This conformational transition enables the developed NPCS nanoprobe functioning as a pH sensor in the range of 4.0−7.5 (Figure 3a and b), which is suitable for monitoring the pH changes intracellularly and extracellularly. Additionally, the developed pH-responsive nanoprobe can be used to produce ratiometric images and thus discriminate the variation in environmental pH at different length scales examined by IVIS (Figure 3c) or CLSM (Figure 5).

Choosing specific fluorophores (donor and acceptor) for FRET-based imaging probes must consider their respective excitation and emission ranges. In our approach, several FRET pairs, not limited by fluorophore wavelengths, may be used to conjugate on NPCS to perform the energy transfer in response to their underlying conformation transition in mapping the environmental pH changes based on the needed experimental conditions for biological applications.

CONCLUSIONS

In conclusion, we successfully developed a dual-emission pH-responsive nanoprobe made of Cy3-/Cy5-labeled NPCS NPs. The change from a weakly charged, globule construction at high pH to a highly charged, expanded coil structure in the network clusters formed at low pH enables the prepared NPs to act as a simple switch off (suppress FRET) or on (gain FRET) in response to changes in the environmental pH, thus may be used to probe the intracellular acidic organelles, such as early/late endosomes and lysosomes. Additionally, this technique may have the potential to localize diseases involving environmental pH changes and hence facilitate diagnosis and therapy.

EXPERIMENTAL SECTION

Materials. Chitosan (CS, viscosity 5 mPa · s, 0.5% in 0.5% acetic acid at 20 °C, MW 50 kDa) with a degree of deacetylation of approximately 85% was purchased from Koyo Chemical Co. Ltd. (Tokyo, Japan). Palmitic acid *N*-hydroxysuccinimide ester was obtained from Sigma-Aldrich (St. Louis, MO). *N*-hydroxy-succinimide (NHS)-functionalized cyanine 3 (Cy3−NHS), cyanine 5 (Cy5−NHS), and fluorescein (fluorescein−NHS) were acquired from Amersham Biosciences (Piscataway, NJ) and Thermo Scientific (Chicago,

IL), respectively. All other chemicals and reagents used were of analytical grade.

Synthesis of NPCS. A mixture of CS (1 g) and aqueous acetic acid (50 mL, 1% w/v) was stirred for 24 h to ensure total solubility. The pH was adjusted to 6.0 by slow addition of 1 N NaOH, and the final volume of CS solution was 100 mL. A solution of palmitic acid *N*-hydroxysuccinimide ester (0.1, 0.2, 0.3, or 0.4 g) in absolute ethanol was added dropwise to the CS solution at 98 °C and reacted for 36 h. Subsequently, the prepared solution was cooled to room temperature, and then acetone was added. The solution was precipitated by adjusting its pH value to 9.0. The precipitate (NPCS) was then filtered, washed with an excess of acetone, and air dried. The synthesized NPCS was analyzed by the proton nuclear magnetic resonance (^{1}H NMR) and Fourier transformed infrared (FT-IR) spectroscopy, and the results were presented in our previous report.[16] Additionally, the degree of substitution (DS) on NPCS was determined by the ninhydrin assay[28] and the potassium polyvinylsulfate (PVSK) titration method.[29]

Preparation and Characterization of NPCS NPs. The synthesized NPCS was dissolved in 1% aqueous acetic acid, and its pH value was adjusted to 4.0 by adding a few drops of 1 N NaOH under magnetic stirring to form NPs. The hydrodynamic radii (R_h) of the prepared NPs at pH 4.5 and 7.4 (adjusted by phosphate buffer) were investigated by dynamic light scattering (ALV/CGS-3, Malvern Instruments Ltd., Worcestershire, U.K.) at varying temperatures.

Preparation of Fluorescent NPCS. Cy3-labeled NPCS (Cy3−NPCS), Cy5-labeled NPCS (Cy5−NPCS), and fluorescein-labeled NPCS (fluorescein−NPCS) were synthesized as per the methods described in the literature.[30] Briefly, a solution of Cy3−NHS, Cy5−NHS, or fluorescein−NHS in DMSO (1 mg/mL) was prepared and added gradually into an aqueous NPCS (2 mg/mL) while stirring; the weight ratio of fluorescent dye to NPCS was kept at 1:50 (w/w). The reaction was maintained at pH 5.5 and stirred continuously for 12 h in the dark. To remove the unconjugated fluorescent dyes, the synthesized Cy3−, Cy5−, and fluorescein−NPCS were dialyzed in the dark against deionized water and replaced on a daily basis until no fluorescence was detected in the supernatant. The resultant Cy3− and Cy5−NPCS and fluorescein−CS were lyophilized in a freeze dryer.

FRET Measurements. Fluorescent NPs were prepared by mixing an equal volume of aqueous Cy3−NPCS and Cy5−NPCS (1% by w/v) and then sonicated in a bath sonicator using a similar procedure as described above. The emission spectra of the prepared fluorescent (Cy3-/Cy5-labled) NP suspensions (100 μg/mL) at distinct pH values were determined by a fluorescence spectrometer (Spex FluoroMax-3, Horiba Jobin Yvon, Edison, NJ). For FRET measurements, the donor (Cy3) was excited at 520 nm, and the emission spectra of the donor−acceptor were recorded at all wavelengths simultaneously.

Dual-emission images of fluorescent NP suspensions at distinct pH environments were acquired using an IVIS (Xenogen, Alameda, CA). In the study, Cy3-/Cy5-labled NP suspensions (100 μg/mL, 200 μL per well) were loaded in a 96-well plate. The plate was irradiated at a wavelength of 535 ± 15 nm and then imaged with sequential emission filters (580 ± 10 and 680 ± 10 nm bandpass) to obtain unmixed Cy3 and Cy5 images. The composite images of unmixed Cy3 and Cy5 images were then processed using the Living Imaging 3.0 Software.

Endocytosis Pathway. To elucidate the potential cellular uptake pathway of NPCS NPs, the interaction between NPCS NPs (fluorescein-labeled) and cell membranes was investigated by treating cells with different chemical inhibitors and then analyzed by flow cytometry. HT1080 cells were seeded in 12-well plates at 1×10^5 cells/well and were allowed to adhere overnight. Subsequently, cells were preincubated with the following inhibitors individually at concentrations which were not toxic to the cells: 7 μg/mL of chlorpromazine,[19,20] 500 nM wortmannin,[21] 3 mM methyl-β-cyclodextrin (MβCD),[19] or 200 μM genistein.[22] Following the preincubation for 30 min, the inhibitor solutions were removed, and freshly prepared fluorescein-labeled NPCS NPs (10 μg/mL) in media containing the same inhibitor concentrations as those mentioned above were added and further incubated for 2 h. After incubation, the cells were washed three times with PBS, detached by 0.025% trypsin/EDTA, and then transferred to microtubes. Subsequently, cells were resuspended in PBS containing 1 mM EDTA and 2% FBS and fixed in 4% paraformaldehyde. Finally, the cells were introduced into a flow cytometer equipped with a 488 nm argon laser (Beckman Coulter, Fullerton, CA).

Intracellular Trafficking. To study the intracellular trafficking of test NPs, cells were treated with the Cy5-labeled NPCS NPs (50 μg/mL) in the serum-free medium. After incubation at predetermined time points, cells were washed twice with the prewarmed PBS before they were fixed in 4% paraformaldehyde. The fixed cells were investigated using the immunohistochemical stains to identify caveolae, caveosomes, early endosomes, and lysosomes. The primary antibodies used in the study were polyclonal rabbit anticaveolin-1 antibody (Cell Signaling Technology #3238, Beverly, MA), polyclonal rabbit anti-EEA1 antibody (Abcam #ab2900), and monoclonal mouse anti-LAMP2 antibody (Abcam #ab25631). After the primary antibody incubation, the following secondary antibodies were used: Alexa Fluor 488 goat antirabbit IgG (H + L) (Invitrogen #A11034) or Alexa Fluor 488 goat antimouse IgG (H + L) (Invitrogen #A110209). The stained cells were counterstained to visualize nuclei with propidium iodide (PI, Sigma-Aldrich) and examined using CLSM (TCS SL, Leica, Germany). In the study, images of cellular organelles (identified by Alexa Fluor 488), cellular nuclei (stained by PI), and Cy5-labeled NPCS NPs were acquired in optical windows between 500−540, 560−650, and 660−700 nm, respectively (after the excitation at 488, 543, and 633 nm, respectively).

Mapping Spatial pH Changes in Living Cells. To perform the intracellular fluorescence ratiometric imaging, cells were treated with Cy3-/Cy5-labeled NPs as per the procedure used in the intracellular trafficking study. The FRET donor Cy3 was excited at 543 nm, and fluorescence images were monitored in a Cy3 imaging channel (560−600 nm) and a Cy5 imaging channel (660−700 nm). The corresponding pseudocolored ratio images were obtained by analyzing the ratio of the signal intensities of Cy5 to Cy3 imaging channels using ZEN 2009 Light Edition Software.

Acknowledgment. This work was supported by a grant from the National Science Council (NSC 98-2120-M-007-007), Taiwan.

Supporting Information Available: Emission ratios of Cy5/Cy3 as a function of the environmental pH, FRET spectra of Cy3−/Cy5−NPCS-5% and -10%, and confocal images of the intracellular trafficking of NPCS NPs. This material is available free of charge *via* the Internet at http://pubs.acs.org.

REFERENCES AND NOTES

1. Smith, C. A.; Wood, E. J. *In Cell Biology*, 2nd ed; Chapman & Hall: London, 1996.
2. Uchiyama, S.; Makino, Y. Digital Fluorescent pH Sensors. *Chem. Commun.* **2009**, 2646–2648.
3. Coupland, P. G.; Briddon, S. J.; Aylott, J. W. Using Fluorescent pH-Sensitive Nanosensors to Report Their Intracellular Location after Tat-Mediated Delivery. *Integr. Biol.* **2009**, *1*, 318–323.
4. Andreev, O. A.; Dupuy, A. D.; Segala, M.; Sandugu, S.; Serra, D. A.; Chichester, C. O.; Engelman, D. M.; Reshetnyak, Y. K. Mechanism and Uses of a Membrane Peptide that Targets Tumors and Other Acidic Tissues *In Vivo*. *Proc. Natl. Acad. Sci. U.S.A.* **2007**, *104*, 7893–7898.
5. Gallagher, F. A.; Kettunen, M. I.; Day, S. E.; Hu, D. E.; Ardenkjær-Larsen, J. H.; in't Zandt, R.; Jensen, P. R.; Karlsson, M.; Golman, K.; Lerche, M. H. Magnetic Resonance Imaging of pH *In Vivo* Using Hyperpolarized ^{13}C-Labelled Bicarbonate. *Nature* **2008**, *453*, 940–944.
6. Jares-Erijman, E. A.; Jovin, T. M. FRET Imaging. *Nat. Biotechnol.* **2003**, *21*, 1387–1395.
7. Lee, S.; Park, K.; Kim, K.; Choi, K.; Kwon, I. C. Activatable Imaging Probes with Amplified Fluorescent Signals. *Chem. Commun.* **2008**, 4250–4260.
8. Roy, R.; Hohng, S.; Ha, T. A Practical Guide to Single-Molecule FRET. *Nat. Methods* **2008**, *5*, 507–516.
9. Xiao, M.; Reifenberger, J. G.; Wells, A. L.; Baldacchino, C.;

Chen, L. Q.; Ge, P.; Sweeney, H. L.; Selvin, P. R. An Actin-Dependent Conformational Change in Myosin. *Nat. Struct. Biol.* **2003**, *10*, 402–408.
10. Medintz, I. L.; Clapp, A. R.; Mattoussi, H.; Goldman, E. R.; Fisher, B.; Mauro, J. M. Self-Assembled Nanoscale Biosensors Based on Quantum Dot FRET Donors. *Nat. Mater.* **2003**, *2*, 630–638.
11. Medintz, I. L.; Clapp, A. R.; Brunel, F. M.; Tiefenbrunn, T.; Uyeda, H. T.; Chang, E. L.; Deschamps, J. R.; Dawson, P. E.; Mattoussi, H. Proteolytic Activity Monitored by Fluorescence Resonance Energy Transfer through Quantum-Dot-Peptide Conjugates. *Nat. Mater.* **2006**, *5*, 581–589.
12. Wang, H.; Yang, R.; Yang, L.; Tan, W. Nucleic Acid Conjugated Nanomaterials for Enhanced Molecular Recognition. *ACS Nano* **2009**, *3*, 2451–2460.
13. Nguyen, H. D.; Dang, D. T.; van Dongen, J. L. J.; Brunsveld, L. Protein Dimerization Induced by Supramolecular Interactions with Cucurbit[8]uril. *Angew. Chem., Int. Ed.* **2010**, *49*, 895–898.
14. Ghadiali, J. E.; Cohen, B. E.; Stevens, M. M. Protein Kinase-Actuated Resonance Energy Transfer in Quantum Dot Peptide Conjugates. *ACS Nano* **2010**, *4*, 4915–4919.
15. Chen, H. H.; Ho, Y. P.; Jiang, X.; Mao, H. Q.; Wang, T. H.; Leong, K. W. Simultaneous Non-Invasive Analysis of DNA Condensation and Stability by Two-Step QD-FRET. *Nano Today* **2009**, *4*, 125–134.
16. Chiu, Y. L.; Chen, M. C.; Chen, C. Y.; Lee, P. W.; Mi, F. L.; Jeng, U. S.; Chen, H. L.; Sung, H. W. Rapidly *In Situ* Forming Hydrophobically-Modified Chitosan Hydrogels *via* pH-Responsive Nanostructure Transformation. *Soft Matter* **2009**, *5*, 962–965.
17. Kumar, M. N. V. R.; Muzzarelli, R. A. A.; Muzzarelli, C.; Sashiwa, H.; Domb, A. J. Chitosan Chemistry and Pharmaceutical Perspectives. *Chem. Rev.* **2004**, *104*, 6017–6084.
18. Rinaudo, M. Chitin and Chitosan: Properties and Applications. *Prog. Polym. Sci.* **2006**, *31*, 603–632.
19. von Gersdorff, K.; Sanders, N. N.; Vandenbroucke, R.; De Smedt, S. C.; Wagner, E.; Ogris, M. The Internalization Route Resulting in Successful Gene Expression Depends on Both Cell Line and Polyethylenimine Polyplex Type. *Mol. Ther.* **2006**, *14*, 745–753.
20. Perumal, O. P.; Inapagolla, R.; Kannan, S.; Kannan, R. M. The Effect of Surface Functionality on Cellular Trafficking of Dendrimers. *Biomaterials* **2008**, *29*, 3469–3476.
21. Araki, N.; Johnson, M. T.; Swanson, J. A. A Role for Phosphoinositide 3-Kinase in the Completion of Macropinocytosis and Phagocytosis by Macrophages. *J. Cell Biol.* **1996**, *135*, 1249–1260.
22. Manunta, M.; Tan, P. H.; Sagoo, P.; Kashefi, K.; George, A. J. T. Gene Delivery by Dendrimers Operates *via* a Cholesterol Dependent Pathway. *Nucleic Acids Res.* **2004**, *32*, 2730–2739.
23. Parton, R. G.; Simons, K. The Multiple Faces of Caveolae. *Nat. Rev. Mol. Cell Biol.* **2007**, *8*, 185–194.
24. Mayor, S.; Pagano, R. E. Pathways of Clathrin-Independent Endocytosis. *Nat. Rev. Mol. Cell Biol.* **2007**, *8*, 603–612.
25. Snee, P. T.; Somers, R. C.; Nair, G.; Zimmer, J. P.; Bawendi, M. G.; Nocera, D. G. A Ratiometric CdSe/ZnS Nanocrystal pH Sensor. *J. Am. Chem. Soc.* **2006**, *128*, 13320–13321.
26. Suzuki, M.; Husimi, Y.; Komatsu, H.; Suzuki, K.; Douglas, K. T. Quantum Dot FRET Biosensors that Respond to pH, to Proteolytic or Nucleolytic Cleavage, to DNA Synthesis, or to a Multiplexing Combination. *J. Am. Chem. Soc.* **2008**, *130*, 5720–5725.
27. Peng, H. S.; Stolwijk, J. A.; Sun, L. N.; Wegener, J.; Wolfbeis, O. S. A Nanogel for Ratiometric Fluorescent Sensing of Intracellular pH Values. *Angew. Chem., Int. Ed.* **2010**, *49*, 4246–4249.
28. Curotto, E.; Aros, F. Quantitative Determination of Chitosan and the Percentage of Free Amino Groups. *Anal. Biochem.* **1993**, *211*, 240–241.
29. Tôei, K.; Kohara, T. A Conductometric Method for Colloid Titrations. *Anal. Chim. Acta* **1976**, *83*, 59–65.
30. Ho, Y. P.; Chen, H. H.; Leong, K. W.; Wang, T. H. Evaluating the Intracellular Stability and Unpacking of DNA Nanocomplexes by Quantum Dots-FRET. *J. Controlled Release* **2006**, *116*, 83–89.